ACS Catalysis

pubs.acs.org/acscatalysis
Research Article

New Mechanistic Insights into the Copper-Free Heck–Cassar–Sonogashira Cross-Coupling Reaction

Chiara Palladino, Tommaso Fantoni, Lucia Ferrazzano, Beatrice Muzzi, Antonio Ricci, Alessandra Tolomelli, and Walter Cabri*

Cite This: ACS Catal. 2023, 13, 12048–12061
Read Online

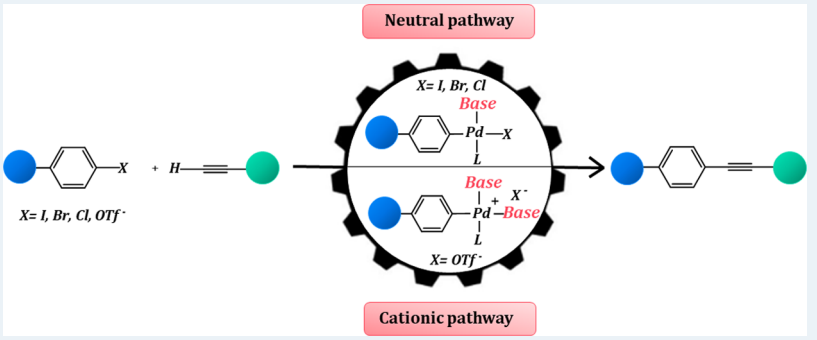

ABSTRACT: The copper-free Heck–Cassar–Sonogashira (HCS) reaction, known since 1975, nowadays represents one of the most powerful methods for C–C bond formation in organic synthesis with several industrial applications. Despite its great success, the mechanism is still under discussion, with several reported possible pathways. To clarify the copper-free HCS reaction mechanism, stoichiometric and catalytic reactions were carried out and monitored by $^{31}P/^{1}H$ NMR spectroscopy, HPLC, and GC chromatography. In particular, the investigation of the role of the base, mimicking the real catalytic conditions, highlighted the fact that secondary amines rapidly induce precatalyst reduction and decrease the energy barrier for the alkyne carbopalladation step. The results supported the mechanism via direct coordination of the terminal alkyne on the oxidative addition complex. Depending on the palladium counterion, and independent of the solvent, aromatic substitutions, temperature, and terminal alkyne substitution, these studies support two different pathways: with halides, a neutral route, and with the triflate, a cationic one.

KEYWORDS: *Heck–Cassar–Sonogashira reaction, copper-free, palladium, mechanism, cross-coupling reaction*

INTRODUCTION

With the exception of the Buchwald–Hartwig amination, the main palladium-catalyzed cross-coupling reactions were discovered in the 1970s.[1] However, only in the new millennium, these catalytic reactions have been deeply investigated, resulting in an incredible increase in publications, as well as patents and industrial applications.[2] The Suzuki–Miyaura[3] cross-coupling reaction is the most explored, followed by the Heck[4] and the Heck–Cassar–Sonogashira (HCS)[5] reactions. In particular, the last ones consist of the palladium-catalyzed substitution of a terminal alkyne hydrogen with an aromatic ring (Scheme 1),[6] and several applications in the pharma industry have been reported.[7]

In the beginning of 1975, Heck[5a] and Cassar[5b] independently published the palladium-catalyzed coupling of aryl halides with alkynes using different bases, solvents, and temperatures (sodium methoxide/dimethylformamide (DMF)/50 °C and neat triethylamine/100 °C, respectively). A few months later, Sonogashira[5c] reported a similar protocol under milder conditions, using neat diethylamine at room temperature, with CuI as the cocatalyst. The presence of the Cu(I) salt allowed the reaction to undergo complete conversion with aryl iodides even at room temperature. Sonogashira suggested the involvement of copper salts in the formation of complex **C** as a critical step of the catalytic cycle. Several scientists have studied the nature of the Cu(I)–Pd(II) transmetalation process, and the most recent mechanism is the one outlined in Figure 1a.[8] There is a general consensus on the fact that the Sonogashira protocol is centered on a transmetalation (**TM**) step from a copper(I) alkyne complex **Fa** or **Fb** and the Pd(II) oxidative addition complex **B**. Understanding the reaction mechanisms leads to the development of efficient protocols by optimizing ligands, counterions, solvent, and the base. This

Received: June 18, 2023
Revised: August 3, 2023

Scheme 1. General Scheme of the HCS Reaction

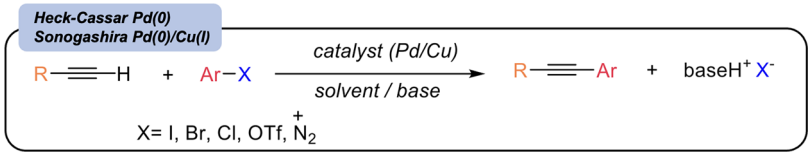

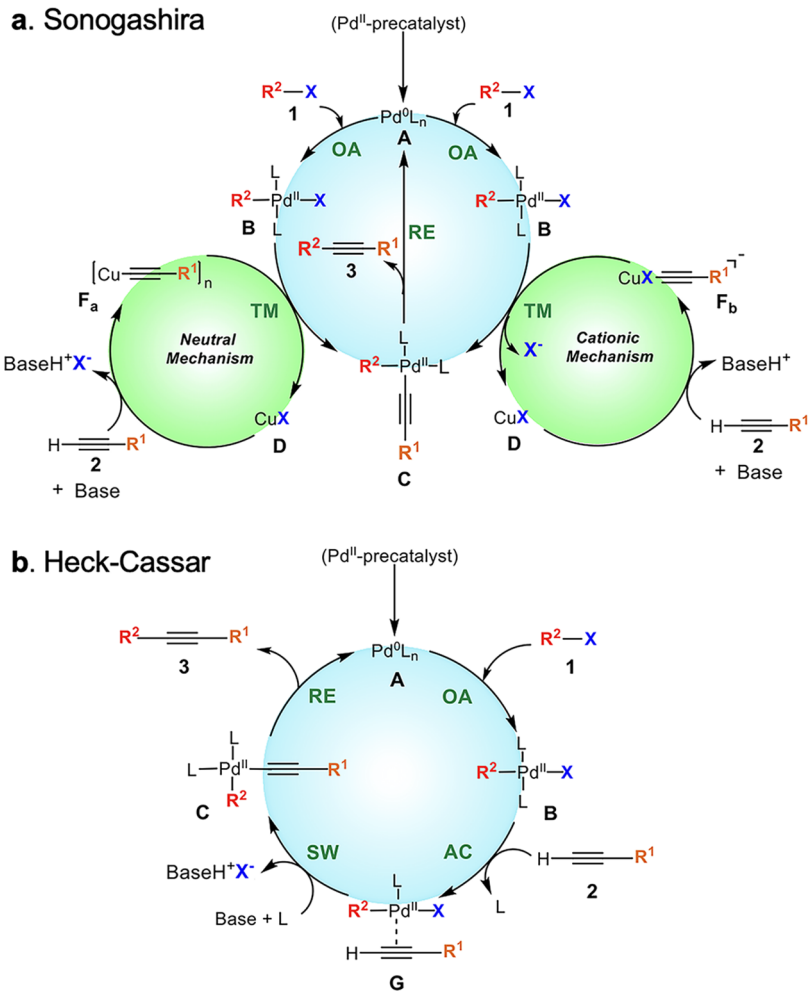

Figure 1. General mechanisms of the Sonogashira (a) and Heck−Cassar (b) protocols.

knowledge enables chemists to avoid byproduct formation, to increase the atom economy, and to save time and chemicals.

The general mechanism of the copper-free Heck−Cassar protocol is described in Figure 1b, but the coordination of the alkyne is still a matter of investigation for several research groups.

Heck−Cassar Protocol Mechanism. The first step in the HCS reaction mechanism, as for all cross-coupling reactions, is the oxidative addition (**OA**) of the Aryl−X onto the Pd(0) complex. This step has been extensively studied by several research groups and for this reason was not investigated in this paper.[9] Harvey and co-workers[9a] carried out DFT calculations and reported that, depending on the ligand, the reactive Pd(0) species can be Pd(0)L or Pd(0)L_2. Moreover, the presence of anionic palladium species, postulated by Amatore and co-workers, such as [Pd(0)L_2X], can play a role in the presence of halides.[9b] However, for the sake of clarity, in the reaction schemes, we considered the Pd(0)L_2 complex as the reactive Pd(0) species when using the triphenylphosphine (PPh_3) ligand and **B**, both as trans isomers. In fact, the **B**cis complex, coming from the **OA**, isomerized to **B**trans, which is more stable by 4.9 kcal with PPh_3 as the ligand and iodide as the halide[10] (see Supporting Figure S184). **B**trans was detected in the reaction mixtures and synthetized. Similarly, the reductive elimination **RE** was not part of this study.

The mechanistic hypothesis of the Heck−Cassar protocol has been intensively studied by several scientists. In 1975, Heck proposed a mechanism where the oxidative addition complex generates the σ-complex **C** by the direct reaction with the deprotonated acetylene.[5a] A simple comparison of the high pK_a of the acetylene (the pKa of phenylacetylene is >20) with the bases generally used does not support this hypothesis.[11] In 2003, Soheili and co-workers at Merck proposed a mechanism where the acetylene, entering the metal coordination sphere, generates the π complex **G**, which, after π/σ (**G**/**C**) switching promoted by the base, efficiently produces the coupling product (Figure 1b).[12] A few years later, Mårtensson's studies supported the Soheili deprotonation mechanism, ruling out the

https://doi.org/10.1021/acscatal.3c02787
ACS Catal. 2023, 13, 12048−12061

potential involvement of a carbopalladation step and proposing an anionic or a cationic coordination process.[13] Later, scientific efforts devoted to shedding light on the Heck−Cassar protocol mechanism were mainly centered on the nature of the π/σ switching and, in addition to the anionic and cationic coordination−carbopalladation step, an ionic pathway was also proposed (Figure 2).[10b] On examination of the DFT data,

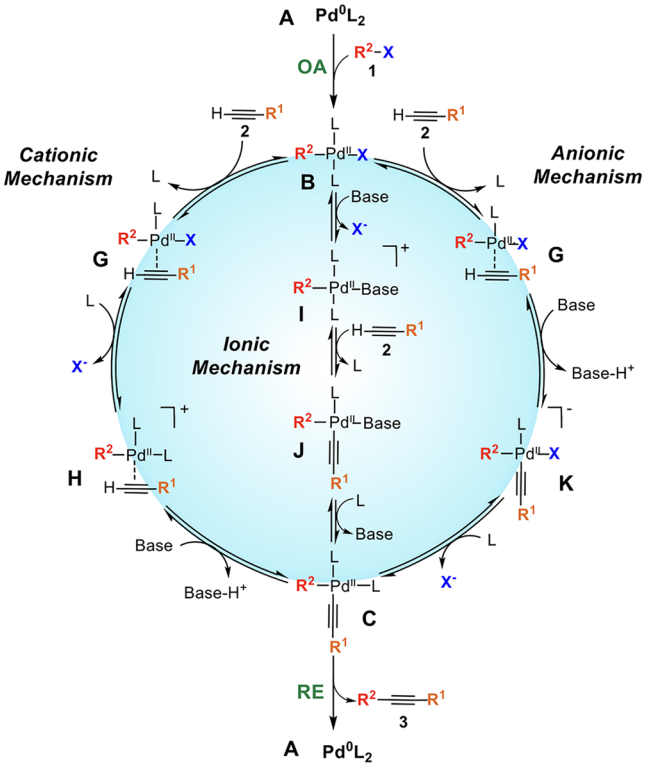

Figure 2. Heck−Cassar protocol based on direct coordination of the alkyne, via cationic, anionic, and ionic routes.

the energy barriers did not look very different considering the standard operational conditions in polar aprotic solvents at a temperature of >60 °C. In addition, the different coordination−carbopalladation processes appear to be a function of several factors, such as the nature of the leaving group, the pK_a of the alkyne, the solvent, and the strength and nucleophilicity of the base. In 2018, Košmrlj and co-workers proposed a general mechanism for the Heck−Cassar protocol based on a second cycle of palladium, as shown in Figure 3.[14] The mechanism was supported by DFT calculations, kinetic studies, and ^{31}P NMR analysis of intermediate complexes. The model consists of two distinct palladium cycles and assumes a Pd(II)−Pd(II) transmetalation (**TM**) process, similar to that of the Sonogashira coupling between the oxidative addition complex **B** and the copper(I) alkyne complex **F** (compare Figure 1a and Figure 3).

Based on the Pd(II)−Pd(II) **TM** in Figure 3, the main side product should be the homodimer **4** generated from complex **M** via a simple reductive elimination (**RE**) process. However, this hypothesis was not in line with our findings.[15] In fact, we designed a green sustainable palladium-catalyzed reaction process using green solvents and *N*,*N*,*N*′,*N*′-tetramethyl guanidine (TMG) as the base, in the presence of different phosphines. Under these conditions, the alkyne homodimer **4** was never observed, even by GC-MS. However, when the

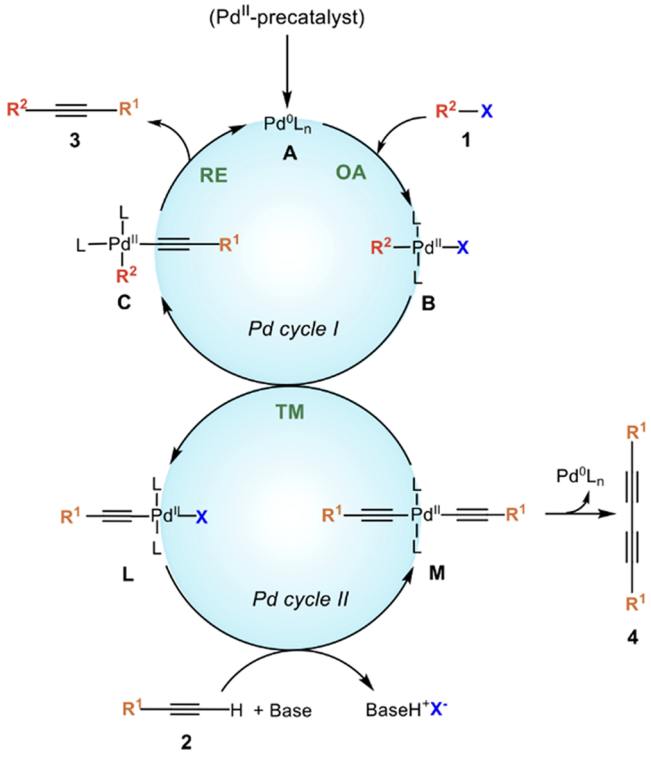

Figure 3. Heck−Cassar protocol based on the Pd(II)−Pd(II) transmetalation mechanism.

oxidative addition step to generate **B** was inefficient, the corresponding enyne, originating from self-hydroalkynylation, was observed. However, the formation of this side product was easily controlled by the slow addition of the alkyne.[15b] The self-hydroalkynylation is the starting point of the oligomerization process. These observations matched with the results reported by Buchwald in 2003[16] and triggered this investigation on the Heck−Cassar protocol, which focuses the attention on the fate of the alkyne under both stoichiometric and catalytic conditions.

Several parameters must be considered in order to control the reaction, such as the ligand, base, solvent, leaving group, concentration, and temperature. The highly reactive palladium species that are generated under the cross-coupling operative conditions can also promote parallel side reactions that could completely change the outcome. Monitoring the reaction through ^{31}P NMR, HPLC, GC, and DFT calculations, the target of this study was to shed light on the Heck−Cassar protocol mechanism under operative conditions.

RESULTS AND DISCUSSION

Pd(II) Precatalyst Reduction. A rapid and complete precatalyst reduction is critical for an efficient process. Therefore, we investigated the base, ligand, and solvent effects on the reduction of $(PPh_3)_2PdCl_2$. The stoichiometry of the reaction requires one molecule of water and generates one molecule of triphenylphosphine oxide. Three bases used in the HCS reaction, i.e., TMG, pyrrolidine (PYR), and triethylamine (TEA), were tested in two different solvents, $CDCl_3$ and DMF-d_7 (Table 1).[17] PYR and TEA are standard bases for the HCS reaction, while TMG was introduced by Cabri et al. only in 1998.[18] Using ^{31}P NMR, we observed that the nature of the base affects the reduction process. TMG, with a high pK_a (23.3 in acetonitrile),[19] was more efficient than PYR in reducing the

https://doi.org/10.1021/acscatal.3c02787
ACS Catal. 2023, 13, 12048−12061

Table 1. Evaluation of Base and Ligand Effects on $(PPh_3)_2PdCl_2$ Reduction to Pd(0)[a]

entry	base	solvent	conv (%)	+PPh_3[b] conv (%)
1	TMG	DMF-d_7	64	100
2	TMG	$CDCl_3$	85	100
3	PYR	DMF-d_7	31	100
4	PYR	$CDCl_3$	65	100
5	TEA	DMF-d_7	0	0[c]
6	TEA	$CDCl_3$	0	0[c]

[a]Reactions were carried out at room temperature with 0.013 mmol of precatalyst and 0.026 mmol of base in 600 μL of solvent for 10 min. Conversions of Pd(II) into Pd(0) were calculated by ^{31}P NMR. [b]Two equivalents of triphenylphosphine were added. [c]The quantitative formation of **M** was observed.

precatalyst (entries 1 and 2 versus entries 3 and 4, respectively, Table 1) at room temperature.

Interestingly, in the presence of an excess of PPh_3 for entries 1−4, the conversion of $(PPh_3)_2PdCl_2$ into Pd(0) complexes was completed in a few minutes (see Supporting Figures S12, S14−S16).

Route A (Scheme 2) is very efficient, and the base affects the reduction process, probably by increasing the phosphine mobility, and when extra quantities of PPh_3 are present, the Pd(II) reduction is fast and complete. On the contrary, TEA was not able to reduce the precatalyst via phosphine oxidation at room temperature (entries 5 and 6) and the addition of phenylacetylene **2a** led to the quantitative formation of complex **M** following route B (see Supporting Figures S17−S18).

Catalytic Cross-Coupling Reactions. The Heck−Cassar copper-free mechanism was studied using a standard protocol: reacting 4-NO_2PhI $\mathbf{1}_{NO2}$ with 1.1 equiv of phenylacetylene **2a**, 2 equiv of the base, and 20 mol% precatalyst $(PPh_3)_2PdCl_2$. The presence of the nitro substituent on the aromatic ring of aryl iodide $\mathbf{1}_{NO2}$ is able to slow down the **RE** step and increase the chances of detecting intermediate complexes of the catalytic cycle. The Pd(II) complexes $\mathbf{B}^{\mathbf{I}}_{\mathbf{NO_2}}$, **C**, **M**, and **L** (Figure 3) were individually synthetized according to previously reported procedures.[14] For this purpose, only TMG and PYR were screened as the base, while TEA was not tested, because of its inefficiency in generating Pd(0) species at room temperature. Independent of the bases or solvents used, it is possible to observe the formation of a small amount of **M**. Nonetheless, with the addition of PPh_3, which accelerates the Pd(II) reduction, complex **M** was not detected by ^{31}P NMR, regardless of the organic base (TMG, PYR) and solvent (DMF-d_7, $CDCl_3$) used (see Supporting Figures S22−S25). In Figure 4, the ^{31}P NMR of the reaction with TMG as the base, with and without additional quantities of PPh_3, is reported.

Complex **M** was formed and detected only when the reduction of the Pd(II) precatalyst was inefficient. Accordingly, when using palladium tetrakis triphenylphosphine (Pd-(PPh3)$_4$) as a catalyst, **M** was never detected (see Supporting Figures S26-S28).

The potential formation of palladium nanoparticles during the reduction of the precatalyst or the cross-coupling process, which could theoretically interfere with the experiments, was ruled out by specific experiments (see Supporting Figures S164−S169).

Side Reactions. The primary objective of the experiments described in Table 2 was the evaluation of the stability of critical Pd(II) complexes at different temperatures in $CDCl_3$ and DMF-d_7, monitoring the formation of the desired coupling product **3a** and the homocoupling **4a**, within a 30 min timeframe.

Complex **M** remained stable at 25 °C in $CDCl_3$ and in DMF-d_7 (entries 1−2 and Supporting Figures S57−S60). However, at 60 °C in $CDCl_3$ (entry 3 and Supporting Figure S62), after 30 min, 30% of complex **M** was converted into the reductive elimination product **4a**. In DMF-d_7, the conversion into **4a** was faster; in fact, already at 40 °C, the conversion was completed within 30 min (entry 4 and Supporting Figures S64−S67). The **OA** complex 4-NO_2-Pd(PPh3)$_2$I $\mathbf{B}^{\mathbf{I}}_{\mathbf{NO_2}}$ in the presence of **M** in $CDCl_3$ generated only a small amount of the cross-coupling product **3a** at 25 °C (entry 5 and Supporting Figure S69), while at 60 °C in DMF-d_7, **M** generated mainly **4a** and only 21% of the coupling product **3a** (entry 6 and Supporting Figures S70−S71). These results showed that the formation of the homocoupling product **4a** is diagnostic of the presence of complex **M**. As expected, the cross-coupling between the oxidative addition complex $\mathbf{B}^{\mathbf{I}}_{\mathbf{NO_2}}$ and **2a** generated exclusively the target product **3a**, entries 7 and 8 (Supporting Figures S73−S75). In other words, the HCS coupling did not require the formation of **M**.

The oxidative addition complex $\mathbf{B}^{\mathbf{I}}_{\mathbf{CH_3}}$ or $\mathbf{B}^{\mathbf{I}}_{\mathbf{NO_2}}$ was stable in $CDCl_3$ or DMF and did not generate, as described by Košmrlj,[14a] the Ar_2PdI_2 and $Ar_2Pd(PPh3)_2$. This last complex is the intermediate of a palladium-catalyzed Ullman-type reaction that follows a completely different path.[20] The Ar−Ar homocoupling product was never detected.

Alkyne Direct Coordination versus Pd(II)−Pd(II) Transmetalation. *Stoichiometric Reactions and Kinetics.* The stoichiometric reactions described in Figure 5 were performed in $CDCl_3$ because of the scarce solubility of **M** in

Scheme 2. Pathway for Pd(II) Precatalyst Reduction

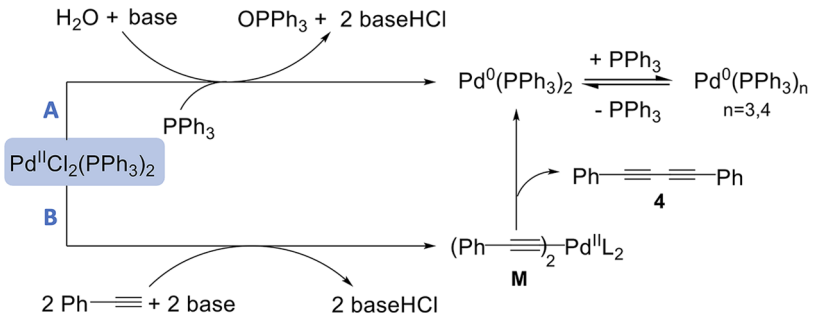

https://doi.org/10.1021/acscatal.3c02787
ACS Catal. 2023, 13, 12048−12061

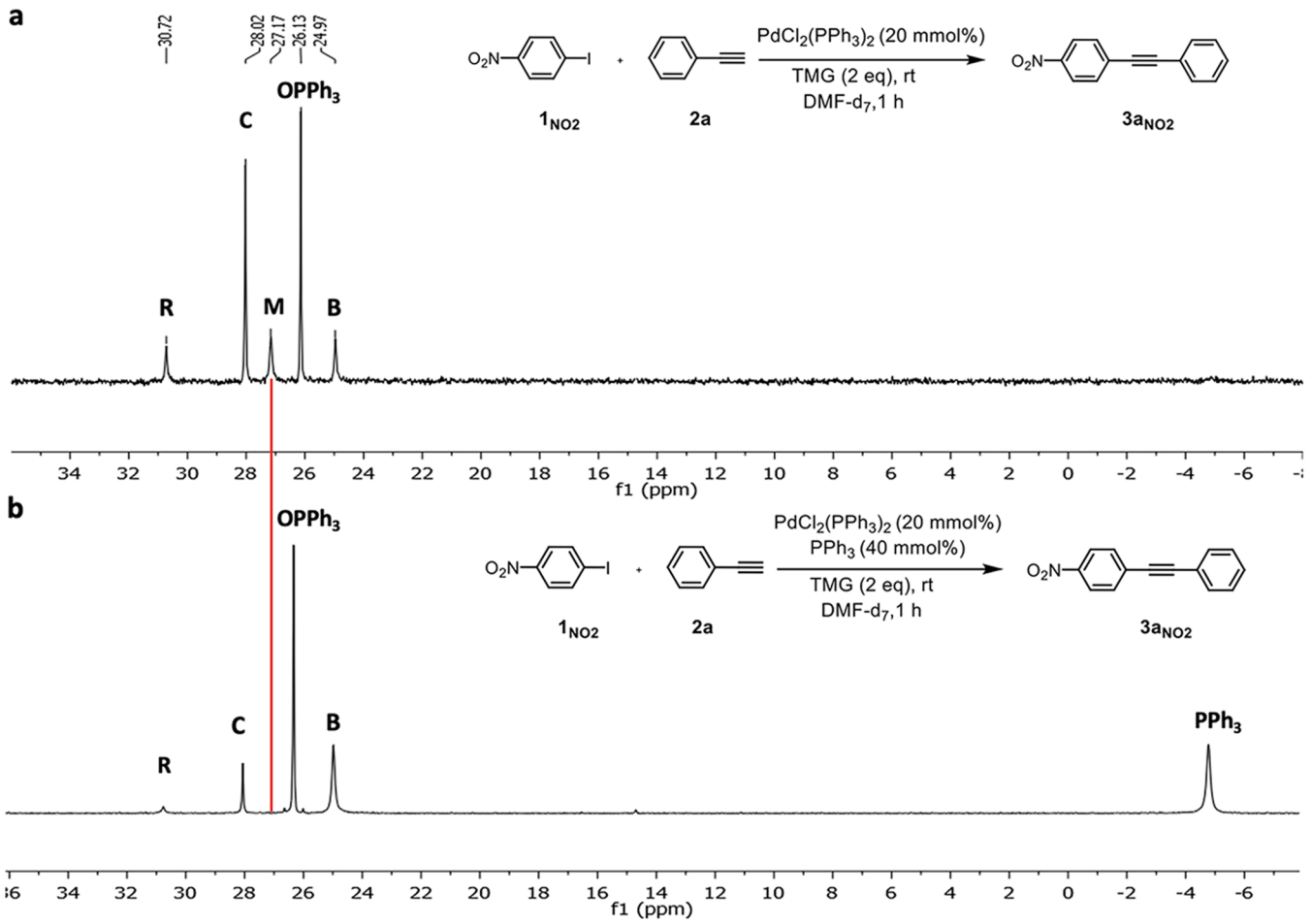

Figure 4. ^{31}P NMR of the HCS reaction carried out with $\mathbf{1}_{NO2}$ (0.5 mmol), **2a** (1.1 equiv), and TMG (2 equiv) as bases in DMF-d_7 (0.5 M) at 25 °C without additional quantities of PPh_3 (a) and with the addition of 2 equiv of PPh_3 (b). Complex **R** is the **OA** complex with the TMG coordinated to palladium.

Table 2. Pd(II) Complex M Stability Studies[a]

entry	solvent	T (°C)	$\mathbf{B}^{I}_{NO_2}$	2a	M	conv (%)	3a/4a[b]
1	$CDCl_3$	25			1	**M** (0)[b]	0/0
2	DMF-d_7	25			1	**M** (0)[b]	0/0
3	$CDCl_3$	60			1	**M** (30)[b]	0/100
4	DMF-d_7	40			1	**M** (100)[c]	0/100
5	$CDCl_3$	25	1		1	$\mathbf{B}^{I}_{NO_2}$ (5)[b]	100/0
6	DMF-d_7	60	1		1	**M** (100)[c]	21/79[d]
7	$CDCl_3$	25	1	1		$\mathbf{B}^{I}_{NO_2}$ (36)[b]	100/0
8	DMF-d_7	60	1	1		$\mathbf{B}^{I}_{NO_2}$ (42)[b]	100/0

[a]All reactions were carried out for 30 min with [C]=0.024 M. For entries 7 and 8, 1.1 equiv of TMG was added. [b]The mixture was analyzed after 30 min by ^{1}H NMR. [c]The mixture was analyzed after 30 min, and the conversion was calculated using ^{31}P NMR. [d]The ratio **3a**/**4a** was determined by HPLC.

other solvents. It is possible to observe that the reaction carried out between complex $\mathbf{B}^{I}_{NO_2}$ and **M** at room temperature in $CDCl_3$ with 1.1 equiv of TMG in triplicate (Figure 5a, green dots) was slower than the couplings $\mathbf{B}^{I}_{NO_2}$/**2a** (red dots) (see Supporting Figures S31 and S36). In order to replicate the identical conditions of Košmrlj et al.,[14a] the reaction was also performed using PYR as the base and 4-CH_3-PhPd(PPh3)$_2$I $\mathbf{B}^{I}_{CH_3}$ as the oxidative addition complex (Figure 5b). The outcomes of the experiments were similar to the one in Figure 5a (see Supporting Figures S44 and S49).

These experiments highlighted that complex **M** was able to promote the cross-coupling, but this pathway was significantly less efficient than the direct reaction between the oxidative addition complex $\mathbf{B}^{I}_{R}$ and the alkyne **2a**, both red dot kinetics in Figure 5a,b. Also, in this case, the direct coordination was faster than the Pd(II)−Pd(II) transmetalation, and in all reactions, the V_{max} was at t=0 (see Supporting Figures S55, S56).

Košmrlj observed a different result[14a] however—the outcome of the stoichiometric reaction can be affected by the solubility of the complexes and the quality of the $CDCl_3$. In all of the experiments described in Figure 5, the palladium complexes were freshly prepared, phenylacetylene was brand new, and $CDCl_3$ was passed over alumina to eliminate any trace of acidity. In fact, chlorides can easily exchange the iodide in the oxidative addition complex.[14b] In addition, these reactions produce Pd(0) species, which can react with $CDCl_3$, generating other side products,[21] or with **2a**, further decreasing the available alkyne.[15b] The direct competition between **M** and **2b** in reacting with the OA complex **B**, described in the next paragraph, avoided any variability or interference of reagents, solvents, or reaction conditions, especially at the beginning of the reaction when the stoichiometry is respected.

https://doi.org/10.1021/acscatal.3c02787
ACS Catal. 2023, 13, 12048−12061

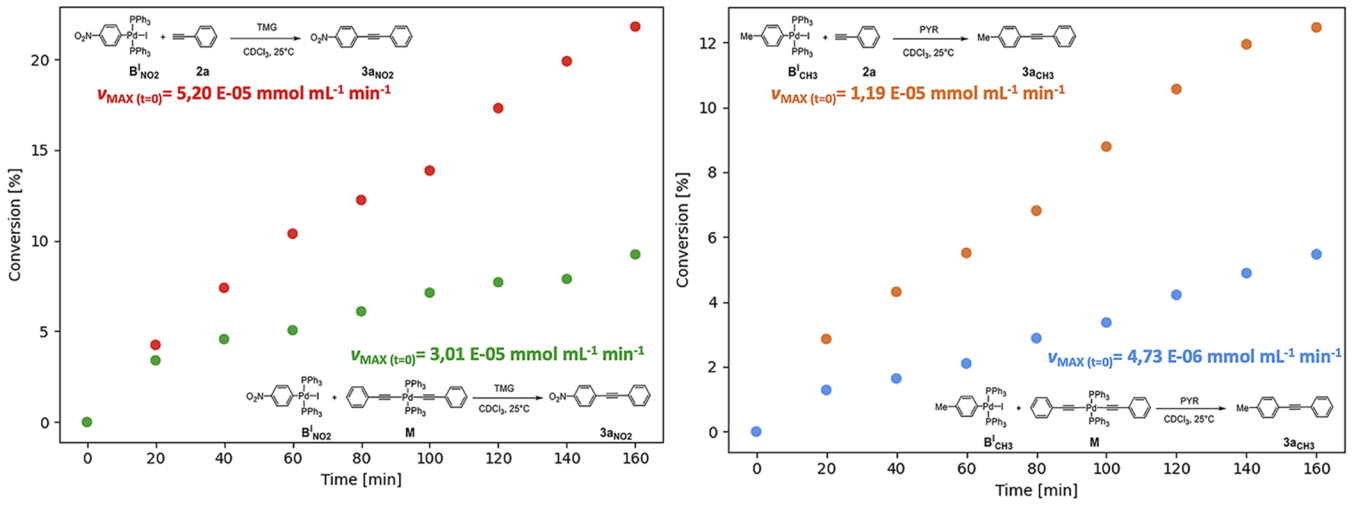

Figure 5. (a) HCS reaction between the oxidative addition complex $\mathbf{B}^{I}_{NO_2}$(0.018 mmol) with **2a** (1 equiv) and TMG (1.1 equiv) and with **M** (1 equiv) in $CDCl_3$ (0.024 M) at 25 °C. (b) HCS reaction between the oxidative addition complex $\mathbf{B}^{I}_{CH_3}$ (0.0095 mmol) with **2a** (1.2 equiv) and Pyr (5 equiv) and with **M** (1.2 equiv) and Pyr (5 equiv) in $CDCl_3$ (0.013 M) at 25 °C.

Scheme 3. Competition between M and 2b in Reacting with Oxidative Addition Complex $\mathbf{B}^{I}_{NO_2}$ and $\mathbf{B}^{I}_{CH_3}$.[a,b]

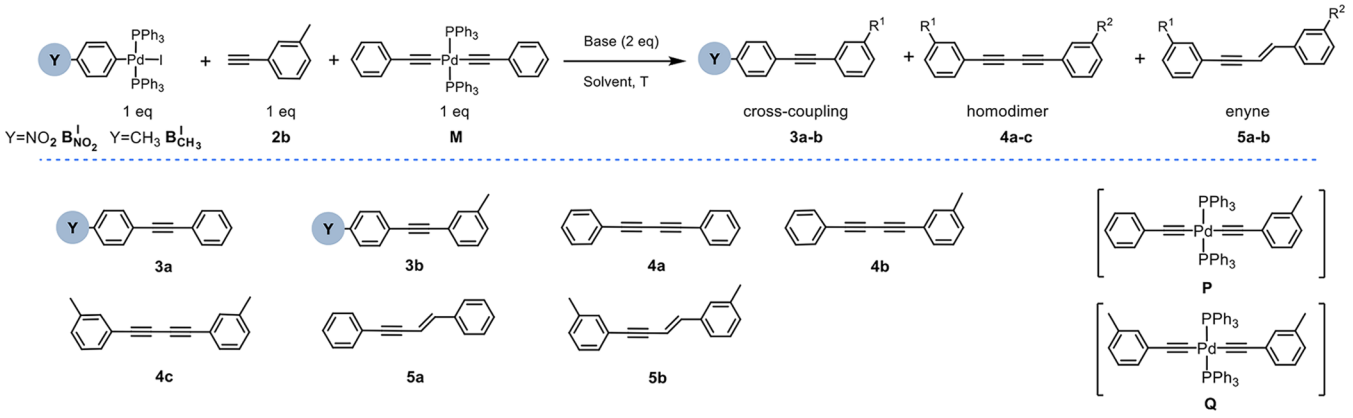

Stoichiometric Competitive Reactions. The competition between the direct coordination process and the Pd(II)−Pd(II) transmetalation one was studied under several reaction conditions with an equimolecular amount of the complexes $\mathbf{B}^{I}_{R}$, **M**, and phenylacetylene **2b** (Scheme 3), which allowed separation of the products coming from the different reaction mechanisms; see Table 3. Compounds **4b**, **4c**, **5a**, and **5b** were not detected.

With the use of a 1/1/1 ratio of $\mathbf{B}^{I}_{R}$/**M**/**2b**, preferential formation of **3b** was observed after 1 h in $CDCl_3$ at 25 °C independent of the substitution on the aromatic ring of $\mathbf{B}^{I}_{R}$ and the base (entries 1−4 and Supporting Figures S76-S88). The use of 10 equiv of **2b**, which mimics the excess of the alkyne in a catalytic reaction, completely suppresses the formation of **3a** (entries 5−6 and Supporting Figures S89−S92). In order to perform the reaction under completely homogeneous conditions and to demonstrate the flexibility of the system, different solvents were screened at 60 °C.

The competition reactions selectively delivered the alkyne cross-coupling product 3b independent of the solvent used, namely, $CDCl_3$, DMF, N-methyl-2-pyrrolidone (NMP), N-buthyl-2-pyrrolidone (NBP), hydroxyethyl-2-pyrrolidone (HEP), tetrahydrofuran (THF), ethanol (EtOH), and toluene (entries 8−15 and Supporting Figures S93−S103), obtaining a complete conversion of $\mathbf{B}^{I}_{NO_2}$ into 3b. Product 3b can be generated only by the direct coordination mechanism, ruling out the Pd(II)−Pd(II) transmetalation process.

In all of the reactions, the only side product detected was the homocoupling product **4a** coming from the reductive elimination **RE** of **M**. In summary, complex **M** is formed only when the palladium precatalyst is not efficiently reduced to Pd(0); however, it is unstable, and by reductive elimination, it generates Pd(0) and the homocoupling product **4a** (see Scheme 2 route B). Accordingly, the homocoupling products were not detected in catalytic reactions performed using Buchwald's[15b] and bidentate phosphine ligands (see Supporting Figures S154−S162), provided that the reduction of the Pd(II) precatalyst was efficiently performed.

In addition, even under conditions where **M** is stable ($CDCl_3$/25 °C), the direct coordination reaction is faster than the Pd(II)−Pd(II) transmetalation one. These data support the direct coordination mechanism hypothesis, which deserves further investigation to establish the role of both the base and the leaving group in directing the reaction toward an anionic, cationic, or ionic mechanism (Figure 2).

Oxidative Addition Complex. $B^{X}_{NO_2}$−*Base Interaction.* In order to understand the behavior of the different Pd(II)

https://doi.org/10.1021/acscatal.3c02787
ACS Catal. 2023, 13, 12048−12061

Table 3. HCS Cross-Coupling Competition Studies, Direct Coordination versus Pd(II)/Pd(II) Transmetalation Process[a]

entry	B	solvent	base	T (°C)	$\mathbf{B}^{I}_{R}$ conv (%)[b]	3a/3b[c]
1	$\mathbf{B}^{I}_{NO_2}$	$CDCl_3$	TMG	25	73	0/100
2	$\mathbf{B}^{I}_{NO_2}$	$CDCl_3$	PYR	25	60	0/100
3	$\mathbf{B}^{I}_{CH_3}$	$CDCl_3$	TMG	25	66	2/98[b]
4	$\mathbf{B}^{I}_{CH_3}$	$CDCl_3$	PYR	25	41	3/97[b]
5[d]	$\mathbf{B}^{I}_{NO_2}$	$CDCl_3$	TMG	25	60	0/100
6[d]	$\mathbf{B}^{I}_{CH_3}$	$CDCl_3$	PYR	25	59	0/100
7	$\mathbf{B}^{I}_{NO_2}$	DMF	TMG	40	100	0/100
8	$\mathbf{B}^{I}_{NO_2}$	DMF	TMG	60	100	0/100
9	$\mathbf{B}^{I}_{NO_2}$	$CDCl_3$	TMG	60	100	0/100
10	$\mathbf{B}^{I}_{NO_2}$	NMP	TMG	60	100	0/100
11	$\mathbf{B}^{I}_{NO_2}$	NBP	TMG	60	100	0/100
12	$\mathbf{B}^{I}_{NO_2}$	HEP	TMG	60	100	0/100
13	$\mathbf{B}^{I}_{NO_2}$	THF	TMG	60	100	0/100
14	$\mathbf{B}^{I}_{NO_2}$	EtOH	TMG	60	100	0/100
15	$\mathbf{B}^{I}_{NO_2}$	toluene	TMG	60	100	0/100

[a]Reactions were carried out with $\mathbf{B}^{I}_{R}$/**M**/**2b** in a 1/1/1 ratio, 1,1 equiv of base with a concentration of 0.13 M under nitrogen for 1 h. [b]Determined by HPLC-MS. [c]Determined by GC-MS. In entries 7−15, the conversion of **M** into **4a** was completed. [d]10 equiv of **2b** were added.

complexes under operative conditions, we carried out ^{31}P analysis of the oxidative addition complexes $\mathbf{B}^{X}_{NO_2}$ with several leaving groups X, namely, I, Br, Cl, or OTf, in the presence of TMG, PYR, or TEA in DMF-d_7. The results are described in Table 4. The base effect was studied using 50/20/10 equiv of the base with respect to the Pd(II) complex $\mathbf{B}^{X}_{NO_2}$ to reproduce the operative conditions. In fact, when using a 1 mol% catalyst, the data showed the impact of 1.1 equiv of the base on the oxidative addition catalyst at different conversions (60, 90, and 99%). The ^{31}P spectra clearly showed that complexes **R** were the dominant Pd(II) species with TMG and PYR (entries 1−6 and Supporting Figures S104−S109), independent of the base excess. The tertiary base TEA was not able to enter the metal coordination sphere (entries 7−9 and Supporting Figure S110).

The value of the equilibrium constant k is generally low and in line with that of Jutand and co-workers.[22] It is clear that the presence of a large excess of base pushes the equilibrium toward the formation of the **R** complexes (Figure 6). Interestingly, with the exception of the chloride complex (entry 6), TMG was always more efficient than PYR in replacing PPh_3 in the Pd(II) coordination sphere (entries 1,2 and 4,5). The introduction of a methoxy group at position 4 of the phenyl iodide favored the formation of complex **R** (entry 10 and Supporting Figure S111).

The results showed that the exchange between the base and the halide does not take place because of the high strength of the Pd(II)−I,Br,Cl bonds.[23] In fact, the formation of complexes **R** is perfectly balanced by the release of free PPh_3 in solution (see Figure 8a $\mathbf{B}^{Br}_{NO_2}$ + 20 equiv of TMG). With oxidative addition complexes coming from aryl halides, the triphenylphosphine release begins upon the addition of the first equivalent of TMG or PYR into the mixture. The ^{31}P NMR spectra showed two or three peaks related to complexes **Ra−c**. With aryl halides, we carried out DFT calculations with TMG as the base, and the data supported the hypothesis that among the different isomers, **Ra** was the most stable (Figure 6). However, the energy difference between **Ra** and **Rb** (1.8−2.3 kcal) is smaller than that between **Rb** and **Rc** (5.3−6.0 kcal), independent of the halide (Figure 6a). Considering the oxidative addition complex generated with triflate as the counterion $\mathbf{B}^{OTf}_{NO_2}$, the formation of complexes **Rd−g** is even more efficient than the one coming from the corresponding aryl halide. Complex $\mathbf{B}^{OTf}_{NO_2}$ is completely dissociated in DMF, and with the addition of the first equivalent of TMG, the formation of two peaks was observed at 27.78 and 19.32 ppm in the ^{31}P NMR spectrum. With the excess of base, only the peak at 27.78 ppm is observed along with the corresponding amount of PPh_3. The complex at 19.32 ppm has only one molecule of TMG attached to the palladium (**Rd,e**), while the complex at 27.78 ppm has two molecules of TMG (**Rf,g**). The cationic complexes **Rd,e** generated from $\mathbf{B}^{OTf}_{NO_2}$ and one molecule of TMG in the coordination sphere of the palladium and those generated with two molecules of TMG (**Rf,g**) have almost the same energy (Figure 6b−c). However, the slightly more stable complexes are those that result from the first substitution of one molecule of TMG in *trans* (**Rd**), and thus, these are the ones that are likely to react in the mechanism giving complexes **Rg** rather than **Rf**.

The mechanisms and energies for the interconversion among the intermediates **Ra**, **Rb**, and **Rc** starting from complex *trans*-$\mathbf{B}^{I}_{NO_2}$ are shown in Figure 7. The only **R** isomer that can be formed from *trans*-$\mathbf{B}^{I}_{NO_2}$ is **Ra**, which is the most stable complex. **Ra** can isomerize to give first **Rb** and then **Rc**. The total energy required to go from **Ra** to **Rb** is 17.5 kcal/mol, while the energy needed to form complex **Rc** from **Rb** is 25.9 kcal. These calculations are in line with the ^{31}P NMR, which shows the presence of a largely predominant **R** isomer and small amounts of the other two when just 10 equiv of base is used (see Supporting Figure S107). On the other hand, when a large excess of base is present, mimicking the reaction conditions, the isomerization is completely inhibited and only the most stable isomer, presumably **Ra**, is detected. This supports the base dissociation mechanism passing through $\mathbf{TS}_{Ra}$.

Alkyne Coordination Step. The intermediate complexes described in Table 4 and in Figure 6 support a coordination process of the alkyne, which is very close to the one postulated for the Heck-type reaction coordination−carbopalladation step.[24] The reaction mechanism, via neutral (**Ra-c**) or cationic (**Rd-g**) complexes, is mainly related to the nature of the counterion in the oxidative addition Pd(II) complex **B**. The coordination of the base and then the alkene/alkyne took place in a neutral complex with the halide counterion (**Ra-c**) and in a cationic complex with the triflate (**Rd-g**).

To the reactions with 20 equiv of base described in Table 4, 20 equiv of **2a** were added. Independent of the counterion, the formation of complex **C** that preceded the **RE** step is a fast process (Supporting Figures S114−S128). In Figure 8, the ^{31}P NMR spectra showed that starting from $\mathbf{B}^{Br}_{NO_2}$, the addition of the base generated a mixture of two main peaks at 27.71 and 31.03 ppm (**Ra-c**), which disappeared after 10 min from the addition of **2a**, forming only complex **C** at 28.03 ppm. We detected the trans isomer of complex C, which is 4 kcal more

https://doi.org/10.1021/acscatal.3c02787
ACS Catal. 2023, 13, 12048−12061

Table 4. Base Effect on the Oxidative Addition Complexes $B^{X}_{NO_2}$, X = I, Br, I, OTf[a]

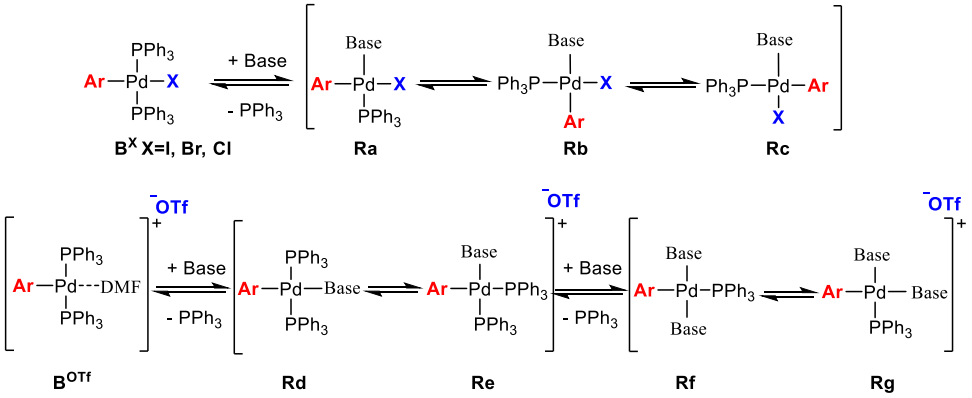

Ar= 4-Y-Ph-

				base/B^{X}_{R} ratio[b]			
entry	X	B^{X}_{R}	base	50 equiv	20 equiv	10 equiv	k
1	I	$B^{I}_{NO_2}$	Pyr	93/7	85/15	68/32	0.182
2	Br	$B^{Br}_{NO_2}$	Pyr	91/9	78/22	68/32	0.099
3	Cl	$B^{Cl}_{NO_2}$	Pyr	93/7	82/18	70/30	0.134
4	I	$B^{I}_{NO_2}$	TMG	100/0	97/3	93/7	0.910
5	Br	$B^{Br}_{NO_2}$	TMG	96/4	85/15	74/26	0.122
6	Cl	$B^{Cl}_{NO_2}$	TMG	87/13	71/29	63/37	0.074
7	I	$B^{I}_{NO_2}$	TEA	0/100	0/100	0/100	
8	Br	$B^{Br}_{NO_2}$	TEA	0/100	0/100	0/100	
9	Cl	$B^{Cl}_{NO_2}$	TEA	0/100	0/100	0/100	
10	I	B^{I}_{OMe}	TMG	>99/1	99/1	94/6	0.306
11	OTf	$B^{OTf}_{NO_2}$	TMG	100/0	100/0	100/0	[c]

[a]The reaction was performed with B^{X}_{R} (0.026 mmol) dissolved in DMF-d_7 (600 μL). [b]Ratios of the complexes and equilibrium constants were calculated using ^{31}P NMR (see the Supporting Information, Paragraph 9). [c]It was not possible to calculate k since the formation of the **R** complex is efficient even with a low amount of base.

stable than the corresponding cis isomer (see Supporting Figure S186). Using the $B^{Br}_{NO_2}$complex, we studied the effect of the alkyne on the reaction outcome. Complex **C** was rapidly generated after 10 min at room temperature, and it was absent after 5 h, while complete conversion to the corresponding HCS products **3a–l** was detected by HPLC (Figure 9 and Supporting Figures S129–S152).

These results further support the observation that the different excess of alkyne, necessary to achieve complete conversions under standard conditions, is not determined by the alkyne reactivity in the HCS coupling. The alkyne coordination and the π/σ switching, necessary to generate **C**, are very fast, and we were unable to detect any intermediate. Therefore, the only possibility was to take advantage of DFT calculations.

DFT Calculations. Density functional theory calculations of the HCS copper-free reaction coordinates were performed with the PBE/def2-TZVP level of theory[25] starting from the oxidative addition complexes, namely, $B^{I}_{NO_2}$ and $B^{OTf}_{NO_2}$, phenylacetylene **2a**, and TMG as a model system to gain molecular-level insights into the mechanism of the alkyne carbopalladation step. According to the experimental data on the effect of the TMG base, two different mechanisms were studied using the iodide and the triflate as counterions: the neutral/anionic pathway via **Ra–c** for the halide species and the cationic/neutral pathway via **Rd–g** for the triflate as the leaving group. **Ra** and **Rg** were selected among the different isomers based on the data described in Figure 6.

The computed Gibbs energy profile for the copper-free HCS reaction starting from the oxidative addition complex $B^{I}_{NO_2}$ is shown in Figure 10a.

The energy of the transition state of the direct carbopalladation of the acetylene on complex $B^{I}_{NO_2}$, without passing through $TS0^{I}$, was found to be 32.0 kcal/mol ($TS1^{PPh3}$). This is the energy necessary for the mechanism involving tertiary amines. With secondary amines, like TMG, the key step of the process is the transformation of $B^{I}_{NO_2}$ into intermediate **Ra** through the displacement of one equivalent of PPh_3 by the base. Our calculations found a barrier of 20.2 kcal/mol ($TS0^{I}$), a difference in energy offset by the excess base that is used in the process. The reaction coordinate was based on **Ra** because it was the most stable isomer; see Figure 6a. The ability of the secondary amine to enter in the coordination sphere of the metal is critical because it lowers the energy required for the acetylene carbopalladation step. The energy required to go from **Ra** to **G** through $TS1^{I}$ is only 22.9 kcal/mol, a process favored by 7.1 kcal over the direct passage from $TS1^{PPh3}$. The calculations therefore reinforce the concept that the carbopalladation step is much faster when passing through complex **Ra**, instead of going directly from complex B^{I}. The step from **Ra** to **G** through $TS1^{I}$ is the rate-determining step of the alkyne carbopalladation process. All subsequent energy

https://doi.org/10.1021/acscatal.3c02787
ACS Catal. 2023, 13, 12048–12061

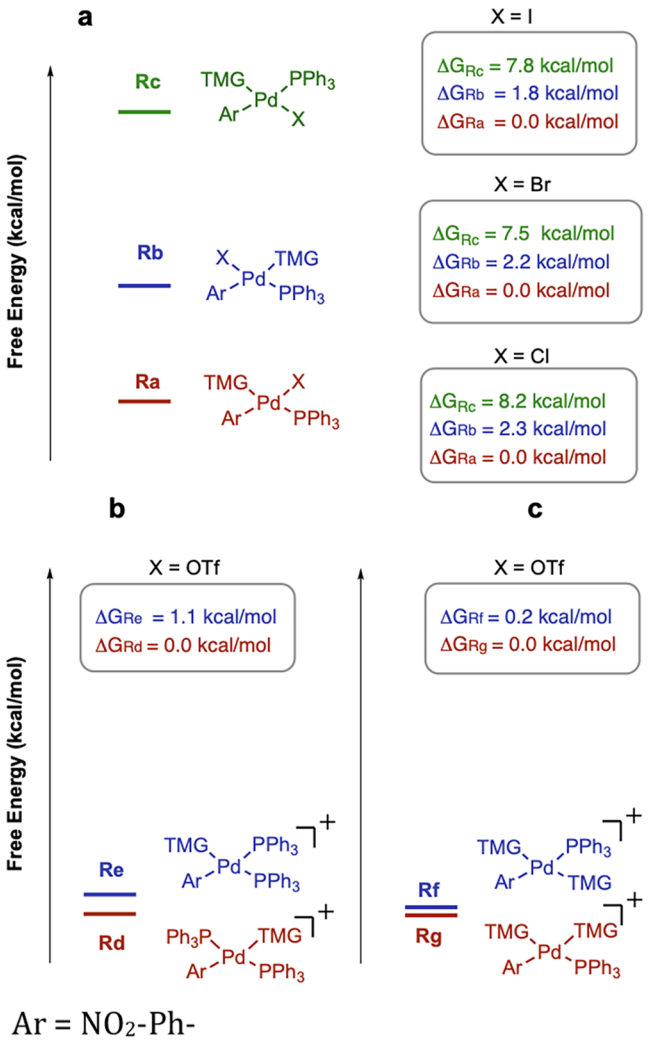

Figure 6. Gibbs energies in DMF (ΔG_{DMF}, kcal mol^{-1}) at 298 K for isomers of complexes **R** with counterion halide (a) and a triflate (b).

barriers from **G** to **C** are lower than the previous transition state from **R** to **G**. The deprotonation of the acetylene is also favored because the base, having just left the complex to make room for the alkyne, remains near the intermediate, facilitating the formation of the anionic complex **N** with an energy barrier of 9.8 kcal/mol. The rupture of the Pd−I bond from the anionic complex **N** requires a low activation energy, and the replacement with PPh_3 is therefore very efficient. In fact, the ΔG between **N** and **TS3**^{I} is only 12.6 kcal/mol, affording the neutral complex **C**, which undergoes reductive elimination with a free energy of 10.8 kcal/mol, giving rise to the coupling product **3** and regenerating the catalyst.

In contrast to the neutral/anionic mechanism that occurs with halides as leaving groups, the HC reaction with triflates is characterized by a cationic/neutral mechanism; see Figure 10b. Currently, there are no data in the literature on DFT calculations for aryl triflates. The Pd−OTf bond is weaker than the Pd−I bond and easily dissociates even in the presence of a ligand such as DMF. For this reason, we started the Gibbs energy profile of the mechanism from $\mathbf{B}_{NO_2}^{OTf}$ with DMF instead of TfO- as the Pd(II) ligand. Based on experimental ^{31}P NMR data, the key initial step was the formation of the complex **Rg** with two TMGs coordinated to the metal. The coordination of the first TMG stabilized the cationic complex by −2.9 kcal/mol (ΔG between $\mathbf{B}_{NO_2}^{OTf}$ and $\mathbf{R}_d$). Similar to the previous mechanism, the second TMG replaces one of the PPh_3 ligands, with a Gibbs free energy of 24.0 kcal/mol, to give the isomer **Rg**, corresponding to the rate-determining step of the process (**TS0**^{OTf}). The carbopalladation of the acetylene into **Rg** takes place with an energy barrier of 20.0 kcal/mol. This transition-state energy barrier from **Rg** to **TS1**^{OTf} is lower than the one previously calculated for the corresponding mechanism step from the iodide complex **Ra**. Interestingly, the average distance between the sp carbons of the alkyne and the palladium complex in **TS1**^{I} was 2.40−2.47 Å, while for **TS1**^{OTf}, a distance of 2.62−2.92 Å was sufficient to activate the C−H bond, creating a lower stressful steric interaction. Analogous to the mechanism outlined for the iodide, after **TS1**^{OTf}, all of the other reaction steps required lower activation energies: the

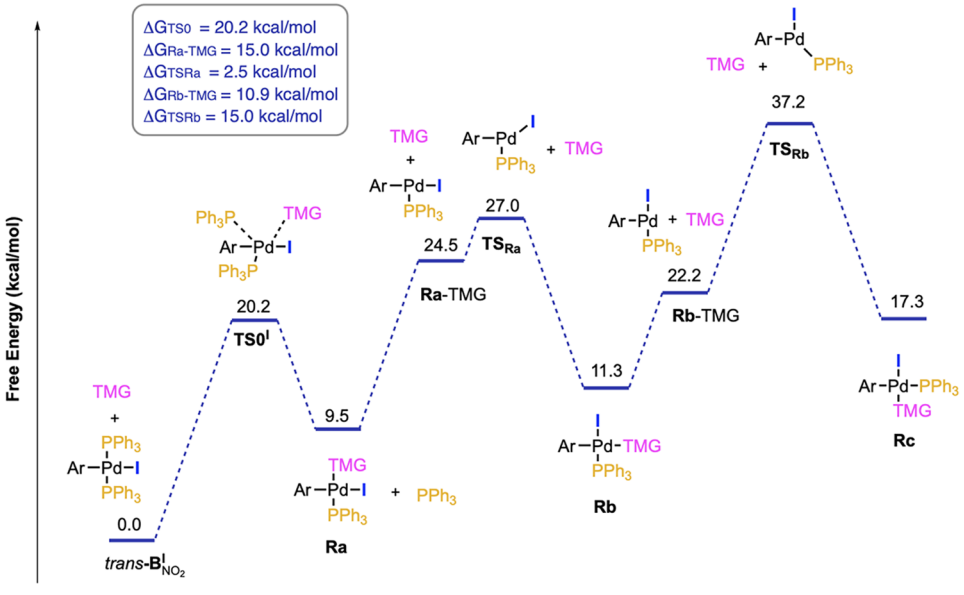

Figure 7. Reaction coordinate of the interconversion among the intermediates **Ra**, **Rb**, and **Rc**.

https://doi.org/10.1021/acscatal.3c02787
ACS Catal. 2023, 13, 12048−12061

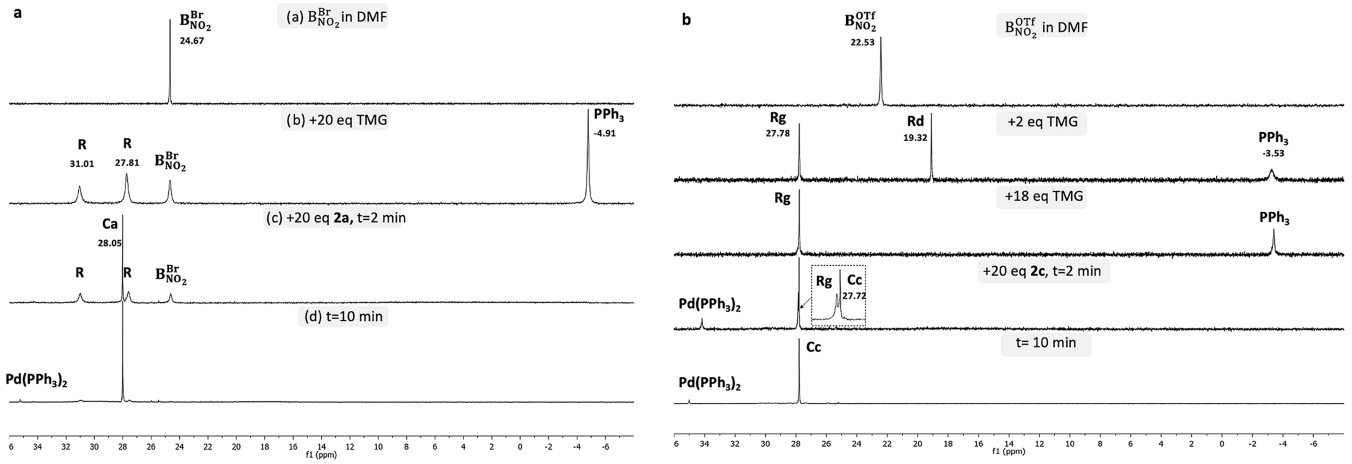

Figure 8. (a) ^{31}P NMR spectra of the complex $\mathbf{B}^{Br}_{NO_2}$ (0.026 mmol) dissolved in DMF-d$_7$ (0.6 mL) followed by the addition of TMG and **2a** at 25 °C. (b) ^{31}P NMR spectra of the complex $\mathbf{B}^{OTf}_{NO_2}$ (0.013 mmol) dissolved in DMF-d$_7$ (0.6 mL) followed by the addition of TMG and **2c** at 25 °C.

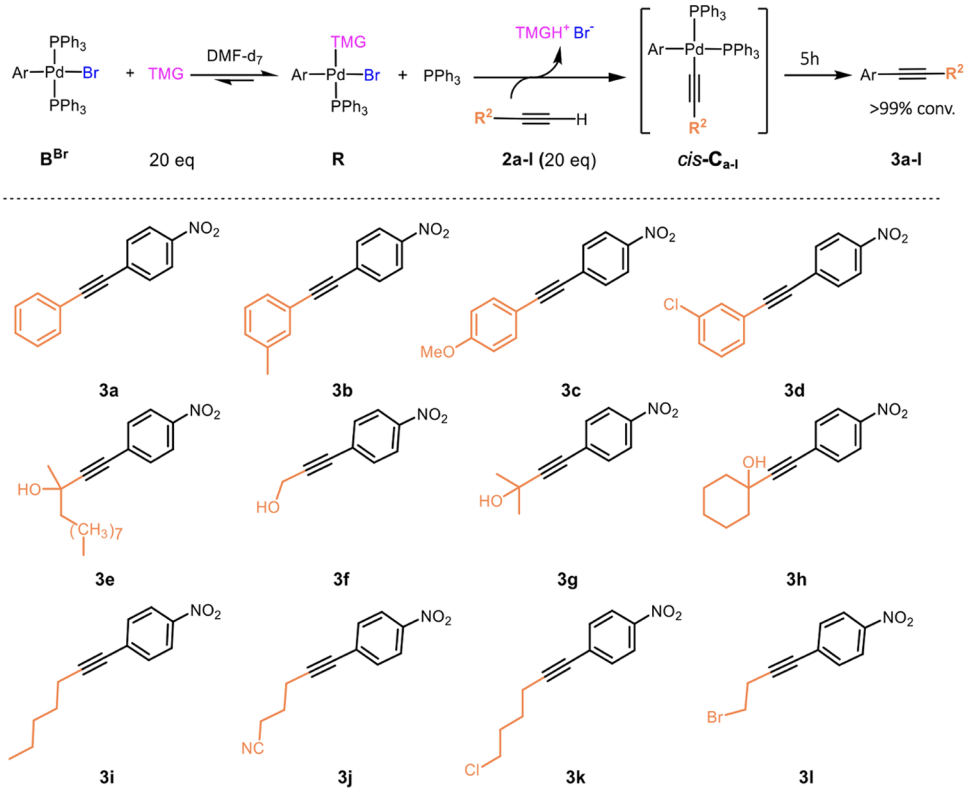

Figure 9. Alkyne carbopalladation into complex $\mathbf{B}^{Br}_{NO_2}$ (0.026 mmol) in 600 μL of DMF-d$_7$.

TMG base, which had just come out of the coordination sphere in $\mathbf{TS1}^{OTf}$, deprotonates the acetylene, favoring the switch from the π complex **S** to the σ complex **T** with an activation energy of only 4.3 kcal/mol. This process is highly favored because it leads to the more stable complex **T** and subsequently to the intermediate **C** through the displacement of TMG by the phosphine with a ΔG energy of 15.8 kcal/mol. The cis/trans isomerization of complex **C** was not discussed since it is not relevant for the reaction mechanism and can only affect the kinetic of the **RE** being the trans isomer more stable and unable to generate the final product.

With both halide and triflate, the DFT calculation showed that the phenylacetylene insertion to the complex **R** is thermodynamically favored over the direct coordination to **B**. This result is consistent with the experimental data described in Figure 8. The formation of complex **R** and **C** is accelerated by the excess of reagents being both bimolecular processes. In fact, the base and the alkyne are always present in large excess with respect to the Pd(II) complexes in a catalytic reaction.

The proposed reaction mechanism is described in Figure 11. In the presence of a halide as a counterion, the direct coordination of the alkyne took place in a neutral complex **G** (Figure 11a), while with triflate, the coordination took place in a cationic complex **S** (Figure 11b).

Concerning the overall reaction rate-determining step, with iodides, the oxidative addition and the coordination of the alkyne transition states have similar energy requirements, around 17−20 kcal/mol.[10b,26] On the contrary, for bromides,

https://doi.org/10.1021/acscatal.3c02787
ACS Catal. 2023, 13, 12048−12061

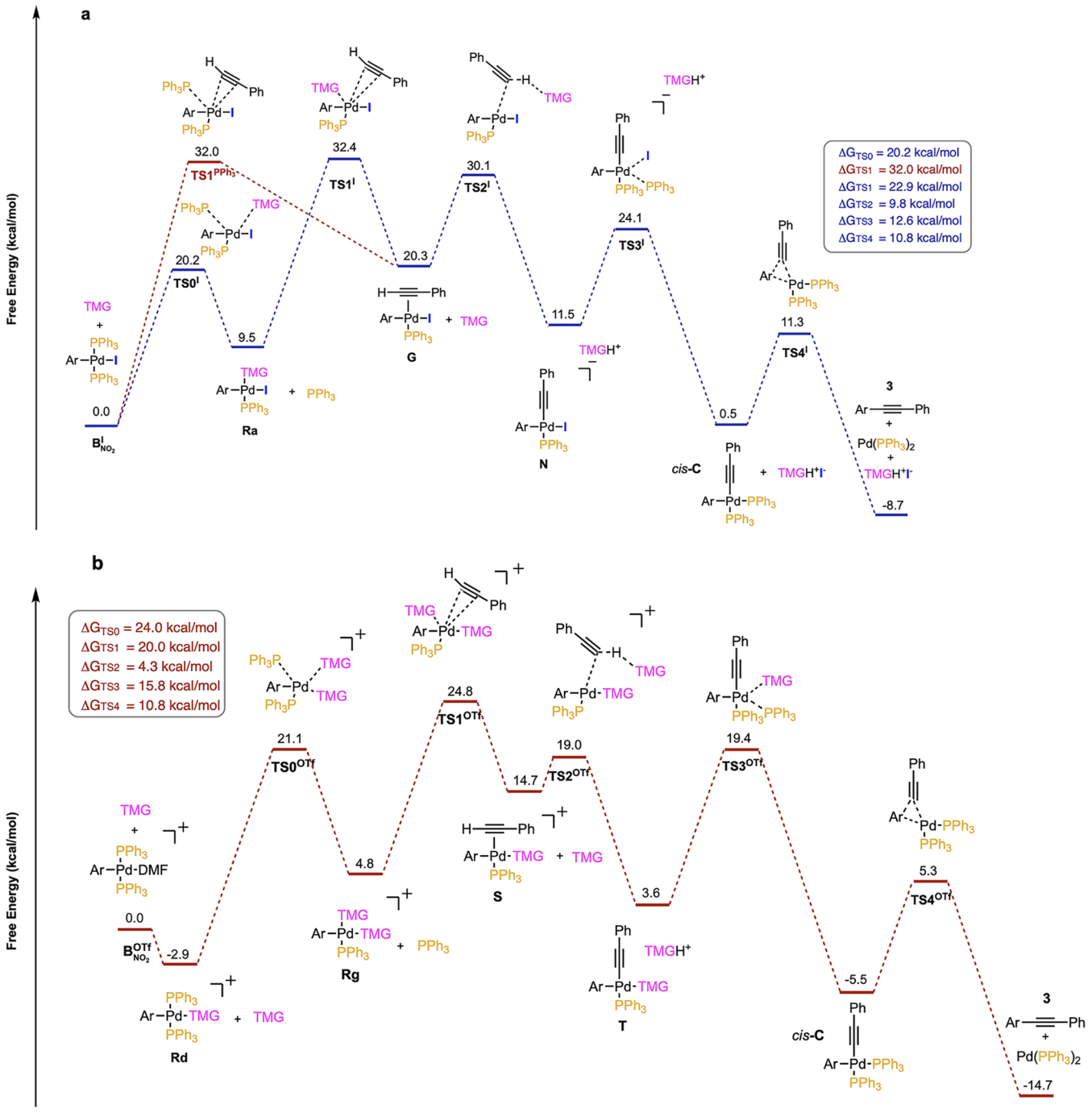

Ar = 4-NO_2-Ph-

Figure 10. DFT-calculation-computed reaction profile and solution-state Gibbs free energies in the DMF (ΔG_{DMF}, kcal mol^{-1}) PBE/def2-TZVP level of theory at 298 K for stationary points of the Heck−Cassar protocol mechanism. (a) Energy profile with iodide as the counterion. (b) Energy profile with triflate as the counterion.

chlorides, and triflates, the oxidative addition is by far the most demanding step, with an energy higher than 30 kcal/mol[27] and higher than that of the acetylene carbopalladation $\mathbf{TS1}^{Br,Cl,OTf}$, which in our calculations turns out to be just 20−23 kcal/mol.

CONCLUSIONS

The investigation of the fate of palladium complexes mimicking operative catalytic conditions was crucial to understand the copper-free HCS reaction mechanism. Palladium species are highly reactive and can undergo side reactions that have the potential to significantly influence the outcome of the reaction and affect data interpretation. In fact, the bis acetylene Pd(II) complex **M** is not involved in a standard HCS copper-free reaction. This complex is unstable and unable to compete with the direct coordination process of the alkyne.

The direct coordination process is faster and more efficient than the Pd(II)−Pd(II) transmetalation mechanism. The outcome is independent of the leaving group, solvent, alkyne,

https://doi.org/10.1021/acscatal.3c02787
ACS Catal. 2023, 13, 12048−12061

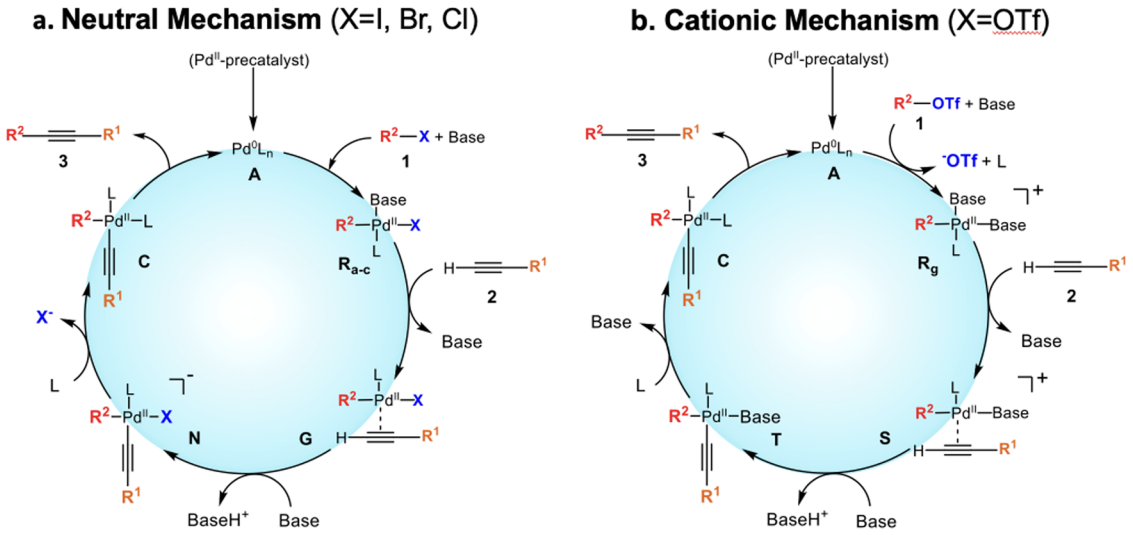

Figure 11. HCS copper-free reaction mechanisms according to the neutral (a) or cationic (b) route.

or temperature used. The homocoupling product in the HCS is diagnostic of the formation of complex **M**, which rapidly generates the active Pd(0) specie. We already reported that with the monodentate Buchwald's ligand or bidentate phosphines the only side product is the enyne, coming from the oxidative addition on the terminal alkyne C–H bond.[15a,b]

The presence of secondary organic amines in the copper-free Heck–Cassar protocol was investigated to understand their fundamental role in promoting precatalyst reduction and entering the coordination sphere of the metal. Experimental results showed that under catalytic conditions, the large excess of secondary amines with respect to the palladium metal and the phosphine ligand affect the Pd(II) complexes and their fate. Theoretical calculations and experimental results showed that there are two different catalytic cycles depending on the type of the involved counterion. When a halide is the counterion, the mechanism involves the coordination of the alkyne in a neutral Pd(II) complex. On the other hand, when the leaving group on the aromatic ring is triflate, which is completely dissociated from the metal, two molecules of the secondary amine enter the palladium coordination sphere, promoting the coordination of the alkyne in a cationic Pd(II) complex. We have reported herein for the first time a DFT calculation on the aryl triflate reactivity in HCS coupling.

This mechanism, which highlights the critical role of the counterion, was found to be similar to the coordination–carbopalladation step involving the alkene in the Heck reaction.[23]

■ ASSOCIATED CONTENT

Supporting Information

The Supporting Information is available free of charge at https://pubs.acs.org/doi/10.1021/acscatal.3c02787.

Synthesis and characterization of complexes, HCS final products, and original data to generate table and DFT calculations (PDF)

■ AUTHOR INFORMATION

Corresponding Author

Walter Cabri − *P4Gi Lab − Projects for Green Innovation, Center of Chemical Catalysis, Department of Chemistry "Giacomo Ciamician", University of Bologna, 40126 Bologna, Italy;* orcid.org/0000-0001-7865-0474; Email: walter.cabri@unibo.it

Authors

Chiara Palladino − *P4Gi Lab − Projects for Green Innovation, Center of Chemical Catalysis, Department of Chemistry "Giacomo Ciamician", University of Bologna, 40126 Bologna, Italy;* orcid.org/0000-0001-8245-9584

Tommaso Fantoni − *P4Gi Lab − Projects for Green Innovation, Center of Chemical Catalysis, Department of Chemistry "Giacomo Ciamician", University of Bologna, 40126 Bologna, Italy*

Lucia Ferrazzano − *P4Gi Lab − Projects for Green Innovation, Center of Chemical Catalysis, Department of Chemistry "Giacomo Ciamician", University of Bologna, 40126 Bologna, Italy;* orcid.org/0000-0002-7083-2211

Beatrice Muzzi − *ICCOM − CNR, Sesto Fiorentino FI I-50019, Italy*

Antonio Ricci − *Fresenius Kabi iPSUM Srl, 45010 Villadose, Italy*

Alessandra Tolomelli − *P4Gi Lab − Projects for Green Innovation, Center of Chemical Catalysis, Department of Chemistry "Giacomo Ciamician", University of Bologna, 40126 Bologna, Italy;* orcid.org/0000-0003-4202-1136

Complete contact information is available at: https://pubs.acs.org/10.1021/acscatal.3c02787

Author Contributions

C.P. and T.F. equally contributed to the paper. The manuscript was written through the contributions of all authors.

Funding

Financial support was provided by the Alma Mater Studiorum, University of Bologna, and Fresenius Kabi. Chiara Palladino's PhD. was part of the MIUR-PON program "PhD 37° cycle grant FSE REACT-EU - A.A. 2021/2022".

Notes

The authors declare no competing financial interest.

■ ACKNOWLEDGMENTS

The authors acknowledge Enrico Faggi S.p.A. for the supply of palladium catalysts. DFT calculations for this work were

performed at CINECA through the Italian SuperComputing Resource Allocation, ISCRA, and the MGCF at UC Berkeley, which is supported by NIH S10OD023532. The authors gratefully acknowledge the Hartwig Group for their assistance.

DEDICATION

This work is dedicated to Richard Heck and Luigi Cassar for their pioneering work in palladium-catalyzed cross-coupling reactions.

REFERENCES

(1) Johansson Seechurn, C. C. C.; Kitching, M. O.; Colacot, T. J.; Snieckus, V. Palladium-Catalyzed Cross-Coupling: A Historical Contextual Perspective to the 2010 Nobel Prize. *Angew. Chem., Int. Ed.* **2012**, *51*, 5062−5085.

(2) Colacot, T. J.; Johansson Seechurn, C. C. C. *Organometallic in Industry*; Wiley-VCH: Weinheim, 2020.

(3) Miyaura, N.; Suzuki, A. Stereoselective synthesis of arylated (E)-alkenes by the reaction of alk-1-enylboranes with aryl halides in the presence of palladium catalyst. *J. Chem. Soc. Chem. Commun.* **1979**, 866−867.

(4) Heck, R. F.; Nolley, J. P., Jr Palladium-catalyzed vinylic hydrogen substitution reactions with aryl, benzyl, and styryl halides. *J. Org. Chem.* **1972**, *37*, 2320−2322.

(5) (a) Dieck, H. A.; Heck, R. F. Palladium catalyzed synthesis of aryl, heterocyclic and vinylic acetylene derivatives. *J. Organomet. Chem.* **1975**, *93*, 259−263. (b) Cassar, L. Synthesis of aryl- and vinyl-substituted acetylene derivatives by the use of nickel and palladium complexes. *J. Organomet. Chem.* **1975**, *93*, 253−257. (c) Sonogashira, K.; Tohda, Y.; Hagihara, N. A convenient synthesis of acetylenes: catalytic substitutions of acetylenic hydrogen with bromoalkenes, iodoarenes and bromopyridines. *Tetrahedron Lett.* **1975**, *16*, 4467−4470.

(6) (a) Schilz, M.; Plenio, H. A Guide to Sonogashira Cross-Coupling Reactions: The influence of Substituents in Aryl Bromides, Acetylenes, and Phosphines. *J. Org. Chem.* **2012**, *77*, 2798−2807. (b) Chinchilla, R.; Nájera, C. *Modern Alkyne Chemistry: Catalytic and Atom-Economic Transformations*; Trost, B. M.; Li, C.-J., Eds.; Wiley-VCH Verlag GmbH & Co. KGaA., 2015; pp 269−297. (c) Alonso, D. A.; Baeza, A.; Chichilla, R.; Gomez, C.; Guillena, G.; Pastor, I. M.; Ramon, D. J. Solid-Supported Palladium Catalysts in Sonogashira Reactions: Recent Developments. *Catalysts* **2018**, *8*, 202. (d) Struwe, J.; Ackermann, L.; Gallou, F. Recent progress in copper-free Sonogashira-Hagihara cross-couplings in water. *Chem. Catal.* **2023**, *3*, No. 100485.

(7) Ponatinib: (a) Huang, W. S.; Metcalf, C. A.; Sundaramoorthi, R.; Wang, Y.; Zou, D.; Thomas, R. M.; Zhu, X.; Cai, L.; Wen, D.; Liu, S.; Romero, J.; Qi, J.; Chen, I.; Banda, G.; Lentini, S. P.; Das, S.; Xu, Q.; Keats, J.; Wang, F.; Wardwell, S.; Ning, Y.; Snodgrass, J. T.; Broudy, M. I.; Russian, K.; Zhou, T.; Commodore, L.; Narasimhan, N. I.; Mohemmad, Q. K.; Iuliucci, J.; Rivera, V. M.; Dalgarno, D. C.; Sawyer, T. K.; Clackson, T.; Shakespeare, W. C. Discovery of 3-[2-(Imidazo[1,2-b]pyridazin-3-yl)ethynyl]-4-methyl-N-{4-[(4-methylpiperazin-1-yl)methyl]-3-(trifluoromethyl)phenyl}benzamide (AP24534), a Potent, Orally Active Pan-Inhibitor of Breakpoint Cluster Region-Abelson (BCR-ABL) Kinase Including the T315I Gatekeeper Mutant. *J. Med. Chem.* **2010**, *53*, 4701−4719. (b) Dong, Z.; Huang, W. S.; Thomas, R. M.; Romero, J. A. C.; Qi, J.; Wang, Y.; Zhu, X.; Shakespeare, W. C.; Sundaramoorthi, R.; Metcalf, C. A.; Dalgarno, D. A.; Sawyer, T. K. (Ariad Pharmaceutical Inc.). U.S. Patent US92789712016. (c) Handa, S.; Jin, B.; Bora, P. P.; Wang, Y.; Zhang, X.; Gallou, F.; Reilly, J.; Lipshutz, B. H. Sonogashira Couplings Catalyzed by Fe Nanoparticles Containing ppm Levels of Reusable Pd, under Mild Aqueous Micellar Conditions. *ACS Catal.* **2019**, *9*, 2423−2431. Erlotinib: (d) Cabri, W.; Oldani, E. (Secifarma). U.S. Patent US59029021999. (e) Caporale, A.; Tartaggia, S.; Castellin, A.; De Lucchi, O. Practical synthesis of aryl-2-methyl-3-butyn-2-ols from aryl bromides via conventional and decarboxylative copper-free Sonogashira coupling reactions. Beilstein. *J. Org. Chem.* **2014**, *10*, 384−393. (f) Chandraratna, R. (Allergan Inc.). U.S. Patent US5602130.1997. Tazarotene: (g) Frigoli, S.; Fuganti, C.; Malpezzi, L.; Serra, S. A Practical and Efficient Process for the Preparation of Tazarotene. *Org. Process Res. Dev.* **2005**, *9*, 646−650. Alectinib: (h) Hughes, D. L. Patent Review of Manufacturing Routes to Recently Approved Oncology Drugs: Ibrutinib, Cobimetinib, and Alectinib. *Org. Process Res. Dev.* **2016**, *20*, 1855−1869 and references therein.. (i) Tolomelli, A.; Ferrazzano, L.; De Nisi, A.; Cabri, W. (Fresenius Kabi & University of Bologna). EP182110362016. Eniluracil: (l) Cooke, J. W. B.; Bright, R.; Coleman, M. J.; Jenkins, K. P. Process research and development of a dihydropyrimidine dehydrogenase inactivator: Large-scale preparation of eniluracil using a Sonogashira coupling. *Org. Process Res. Dev.* **2001**, *5*, 383−386.

(8) (a) Chinchilla, R.; Najera, C. Recent advances in Sonogashira reactions. *Chem. Soc. Rev.* **2011**, *40*, 5084−5121. (b) Rivada-Wheelaghan, O.; Comas-Vives, A.; Fayzullin, R. R.; Lledjs, A.; Khusnutdinova, J. R. Dynamic PdII/CuI Multimetallic Assemblies as Molecular Models to Study Metal−Metal Cooperation in Sonogashira Coupling. *Chem. − Eur. J.* **2020**, *26*, 12168−12179. (c) Wang, X.; Song, Y.; Qu, J. Luo, Mechanistic Insights into the Copper-Cocatalyzed Sonogashira Cross-Coupling Reaction: Key Role of an Anion, Y. *Organometallics* **2017**, *36*, 1042−1048.

(9) (a) McMullin, C. L.; Fey, N.; Harvey, J. N. Computed ligand effects on the oxidative addition of phenyl halides to phosphine supported palladium(0) catalysts. *Dalton Trans.* **2014**, *43*, 13545. (b) Amatore, C.; Azzabi, M.; Jutand, A. Role and effects of halide ions on the rates and mechanisms of oxidative addition of iodobenzene to low-ligated zerovalent palladium complexes $(PPh_3)_2Pd0$. *J. Am. Chem. Soc.* **1991**, *113*, 8376−8384. (c) Amatore, C.; Carré, E.; Jutand, A.; M'Barki, M. A.; Meyer, G. Evidence for the Ligation of Palladium(0) Complexes by Acetate Ions: Consequences on the Mechanism of Their Oxidative Addition with Phenyl Iodide and $PhPd(OAc)(PPh_3)_2$ as Intermediate in the Heck Reaction. *Organometallics* **1995**, *14*, 5605−5614. (d) Liang, H.; Rio, J.; Perrin, L.; Payard, P.-A. Salt-Enhanced Oxidative Addition of Iodobenzene to Pd: An Interplay Between Cation, Anion, and Pd−Pd Cooperative Effects. *Inorg. Chem.* **2022**, *61*, 7935−7944.

(10) There are many mechanisms suggested in literature, including: (a) Casado, A. L.; Espinet, P. On the Configuration Resulting from Oxidative Addition of RX to Pd(PPh3)4 and the Mechanism of the cis-to-trans Isomerization of [PdRX(PPh3)2] Complexes (R) Aryl, X) Halide). *Organometallics* **1998**, *17*, 954−959. (b) García-Melchor, M.; Pacheco, M. C.; Najera, C.; Lledos, A.; Ujaque, G. Mechanistic Exploration of the Pd-Catalyzed Copper-Free Sonogashira Reaction. *ACS Catal.* **2012**, *2*, 135−144.

(11) (a) Streitwieser, A., Jr.; Reuben, D. E. Acidity of hydrocarbons. XXXV. Equilibrium acidities of phenylacetylene and tert-butylacetylene in cyclohexylamine. *J. Am. Chem. Soc.* **1971**, *93*, 1794−1795. (b) Terekhova, M. I.; Petrov, E. S.; Vasilevskii, S. F.; Ivanov, V. F.; Shvartsberg, M. S. Equilibrium CH acidity of arylacetylenes in dimethyl sulfoxide. *Russ. Chem. Bull.* **1984**, *33*, 850−852.

(12) Soheili, A.; Albaneze-Walker, J.; Murry, J. A.; Dormer, P. G.; Hughes, D. L. Efficient and general protocol for the copper-free Sonogashira coupling of aryl bromides at room temperature. *Org. Lett.* **2003**, *5*, 4191−4194.

(13) (a) Ljungdahl, T.; Pettersson, K.; Albinsson, B.; Mårtensson, J. Solvent and base dependence of copper-free palladium-catalyzed cross-couplings between terminal alkynes and arylic iodides: development of efficient conditions for the construction of gold(III)/free-base porphyrin dimers. *J. Org. Chem.* **2006**, *71*, 1677−1687. (b) Ljungdahl, T.; Bennur, T.; Dallas, A.; Emtenäs, H.; Mårtensson, J. Two Competing Mechanisms for the Copper-Free Sonogashira Cross-Coupling Reaction. *Organometallics* **2008**, *27*, 2490−2498.

(14) (a) Gazvoda, M.; Virant, M.; Pinter, B.; Košmrlj, J. Mechanism of copper-free Sonogashira reaction operates through palladium-palladium transmetallation. *Nat. Commun.* **2018**, *9*, No. 4814. (b) Ivančič, A.; Košmrlj, J.; Gazvoda, M. Elucidating the reaction

https://doi.org/10.1021/acscatal.3c02787
ACS Catal. 2023, 13, 12048−12061

mechanism of a palladium-palladium dual catalytic process through kinetic studies of proposed elementary steps. *Commun. Chem.* **2023**, *6*, 51.

(15) (a) Ferrazzano, L.; Martelli, G.; Fantoni, T.; Daka, A.; Corbisiero, D.; Viola, A.; Ricci, A.; Cabri, W.; Tolomelli, A. Fast Heck−Cassar−Sonogashira (HCS) Reactions in Green Solvents. *Org. Lett.* **2020**, *22*, 3969−3973. (b) Fantoni, T.; Bernardoni, S.; Mattellone, A.; Martelli, L.; Ferrazzano, G.; Cantelmi, P.; Corbisiero, D.; Tolomelli, A.; Cabri, W.; Vacondio, F.; Ferlenghi, F.; Mor, M.; Ricci, A. Palladium Catalyst Recycling for Heck-Cassar-Sonogashira Cross-Coupling Reactions in Green Solvent/Base Blend. *ChemSusChem* **2021**, *14*, 2591−2600. (c) Fantoni, T.; Tolomelli, A.; Cabri, W. A translation of the twelve principles of green chemistry to guide the development of cross-coupling reactions. *Catal. Today* **2022**, *397*−*399*, 265−271.

(16) Gelman, D.; Buchwald, S. L. Efficient Palladium-Catalyzed Coupling of Aryl Chlorides and Tosylates with Terminal Alkynes: Use of a Copper Cocatalyst Inhibits the Reaction. *Angew. Chem., Int. Ed.* **2003**, *42*, 5993−5996.

(17) Jutand, A.; Mosleh, A. Rate and Mechanism of Oxidative Addition of Aryl Triflates to Zerovalent Palladium Complexes. Evidence for the Formation of Cationic (α-Aryl)palladium Complexes. *Organometallics* **1995**, *14*, 1810−1817.

(18) Cabri, W.; Oldani, E. Process for the industrial preparation of aminoacetylenes. U.S. Patent US5902902, 1998.

(19) Taylor, J. E.; Bull, S. D.; Williams, J. M. J. Amidines, isothioureas, and guanidines as nucleophilic catalysts. *Chem. Soc. Rev.* **2012**, *41*, 2109−2121.

(20) The palladium catalyzed aryl iodides homocoupling, in other words the Palladium Catalyzed Ullman type reaction, required completely different reaction conditions and several steps oxidative addition/reduction/second oxidative addition to generate $Ar_2Pd(PPh_3)_2$. (a) Jutand, A.; Mosleh, A. Nickel- and Palladium-Catalyzed Homocoupling of Aryl Triflates. Scope, Limitation, and Mechanistic Aspects. *J. Org. Chem.* **1997**, *62*, 261−274. Aryl triflates (b) Hennings, D. D.; Iwama, T.; Rawal, V. H. Palladium-Catalyzed (Ullmann-Type) Homocoupling of Aryl Halides: A Convenient and General Synthesis of Symmetrical Biaryls via Inter- and Intramolecular Coupling Reactions. *Org. Lett.* **1999**, *1*, 1205−1208. Aryl iodides.

(21) (a) Fitton, P.; Johnson, M. P.; McKeon, J. E. Oxidative additions to palladium (0). *Chem. Commun.* **1968**, 6−7. (b) Kaliya, O. L.; Temkin, O. N.; Kirchenkova, G. S.; Smirnova, E. M.; Kimel'fel'd, Y. M.; FLid, R. M. Oxidative coupling of chloroform with tetrakis(triphenylphosphine)palladium. *Russ. Chem. Bull.* **1969**, *18*, 2690−2691.

(22) Jutand, A.; Negri, S.; Principaud, A. Formation of ArPdXL-(amine) Complexes by Substitution of One Phosphane Ligand by an Amine in trans-ArPdX(PPh3)2 Complexes. *Eur. J. Inorg. Chem.* **2005**, *2005*, 631−635.

(23) Henry, P. M. *Palladium Catalyzed Oxidation of Hydrocarbons'*; D. Riedel: Dordrecht: Holland, 1980; pp 11−15.

(24) Cabri, W.; Candiani, I. Recent Developments and New Perspectives in the Heck Reaction. *Acc. Chem. Res.* **1995**, *28*, 2−7.

(25) Kondrashova, S. A.; Polyancev, F. M.; Latypov, S. K. DFT Calculations of 31P NMR Chemical Shifts in Palladium Complexes. *Molecules* **2022**, *27*, 2668.

(26) Ahlquist, M.; Fristrup, P.; Tanner, D.; Norrby, P-O. Theoretical Evidence for Low-Ligated Palladium(0): [Pd-L] as the Active Species in Oxidative Addition Reactions. *Organometallics* **2006**, *25*, 2066−2073.

(27) Schoenebeck, F.; Houlk, K. N. Ligand-Controlled Regioselectivity in Palladium-Catalyzed Cross Coupling Reactions. *J. Am. Chem. Soc* **2010**, *132*, 2496−2497.

https://doi.org/10.1021/acscatal.3c02787
ACS Catal. 2023, 13, 12048−12061